Ray-tracing analysis of crosstalk in multi-core polymer optical fibers

Amaia Berganza,* Gotzon Aldabaldetreku, Joseba Zubia, and Gaizka Durana

Department of Electronics and Telecommunications, University of the Basque Country, ETSI de Bilbao, Alda. Urquijo s/n, E-48013 Bilbao, Spain
**amaia.berganza@ehu.es*

Abstract: The aim of this paper is to present a new ray-tracing model which describes the propagation of light in multi-core polymer optical fibers (MCPOFs), taking into account the crosstalk among their cores. The new model overcomes many of the limitations of previous approaches allowing us to simulate MCPOFs of arbitrary designs. Additionally, it provides us with the output ray distribution at the end of the fiber, making it possible to calculate useful parameters related to the fiber performance such as the Near-Field Pattern, the Far-Field Pattern or the bandwidth. We also present experimental measurements in order to validate the computational model and we analyze the importance of crosstalk in different MCPOF configurations.

OCIS codes: (060.0060) Fiber optics and optical communications; (060.2270) Fiber characterization; (060.2300) Fiber measurements; (060.2310); Fiber optics; (080.0080) Geometric optics.

References and links

1. H. Poisel, and O. Ziemann, "Trends in Polymer Optical Fibers," in *Proceedings of Third GR-I International Conference on New Laser Technologies and Applications. Proceedings of the SPIE* (2003), Carabelas, Alexis; Baldacchini, Giuseppe; Di Lazzaro, Paolo; Zevgolis, Dimitrios, eds. Vol. 5131, pp. 213–219.
2. "Asahi Kasei Co." Available: *http://www.asahi-kasei.co.jp/pof/en/products/multicore.html*.
3. "Asahi Glass Co." Available: *http://www.agc.co.jp*.
4. Y. Koike, "Status of High Speed Plastic Optical Fiber Towards Giga House Town," in *18th International POF Conference. Proceedings* (2009).
5. D. Kalymnios, "Using Plastic Optical Fibre (POF) Cables in Multimedia Applications and Meeting Relevant Recent Standards," in *17th International POF Conference Proceedings* (Santa Clara, Calif., 2008).
6. K. Shimada, H. Sasaki, and Y. Noguchi, "The home networking system based on IEEE1394 and Ethernet Technologies," in *Proceedings of ICCE: International Conference on Consumer Electronics*, (2001). pp. 234–235.
7. N. Ortega-Quijano, F. Fanjul-Vélez, and J. L. Arce-Diego, "Optical crosstalk influence in fiber imaging endoscopes design," Opt. Commun. **283**(4), 633–638 (2010).
8. G. Durana, G. Aldabaldetreku, J. Zubia, J. Arrue, and C. Tanaka, "Coupling losses in perfluorinated multi-core polymer optical fibers," Opt. Express **16**(11), 7929–7942 (2008).
9. A. W. Snyder, "Coupled-Mode Theory for Optical Fibers," J. Opt. Soc. Am. **62**(11), 1267–1277 (1972).
10. A. W. Snyder, and P. McIntyre, "Crosstalk between light pipes," J. Opt. Soc. Am. **66**(9), 877–882 (1976).
11. A. W. Snyder, and J. D. Love, *Optical waveguide theory*, Chapman and Hall, ed. (London, 1983).
12. J.-M. Liu, *Photonic Devices*, Cambridge University Press, ed. (Cambridge, 2005).
13. K. L. Reichenbach, and C. Xu, "Numerical analysis of light propagation in image fibers or coherent fiber bundles," Opt. Express **15**(5), 2151–2165 (2007).
14. G. Aldabaldetreku, J. Zubia, G. Durana, and J. Arrue, "Numerical implementation of the ray-tracing method in the propagation of light through multimode optical fibres," in *POF Modelling: Theory, Measurement and Application*, C.-A. Bunge and H. Poisel, eds. (Books on Demand GmbH, Norderstedt, Germany, 2007), pp. 25–48.
15. N. S. Kapany, *Fiber Optics: Principles and Applications*, Academic Press, ed. (London, 1968).
16. A. H. Cherin, and E. J. Murphy, "Quasi-Ray Analysis of Crosstalk between Multimode Optical Fibers," Bell Syst. Tech. J. **54**(1), 17–45 (1975).
17. M. G. Kuzyk, *Polymer Fiber Optics: Materials, Physics and Applications*, Taylor & Francis, ed. (London, 2007).
18. D. Gloge, and E. A. J. Marcatili, "Multimode Theory of Graded-Core Fibers," J. Bell Syst. Tech. **52**, 1563–1578 (1973).
19. "Hamamatsu Photonics," Available: *http://sales.hamamatsu.com/en/products.php*.

#132325 - $15.00 USD Received 27 Jul 2010; revised 10 Sep 2010; accepted 13 Sep 2010; published 8 Oct 2010

20. S. Sasho, "A Comprehensive Bending Loss Study of Multi-core POF," in *Proceedings of 17th International POF Conference Proceedings* (Santa Clara, Calif., 2008).
21. J. Arrue, J. Zubia, G. Durana, and J. Mateo, "Parameters Affecting Bending Losses in Graded-Index Polymer Optical Fibers," IEEE J. Sel. Top. Quantum Electron. **7**(5), 836–844 (2001).
22. D. Gloge, "Bending loss in multimode fibers with graded and ungraded core index," Appl. Opt. **11**(11), 2506–2513 (1972).

1. Introduction

The interest in Polymer Optical Fibers (POFs) has experienced a tremendous increase in the last years due to the more and more demanding requirements of up-to-date applications such as Local Area Networks (LANs), Fiber To The Home (FTTH) or sensors. Some of the main advantages of POFs in these applications are that they are easy to handle, due to their large core diameter, and that they are flexible, making them easy to lie down, although it is important to keep in mind that bending the fiber increases the total losses in the system [1].

Recently, new kinds of POFs have been developed in order to achieve low bending losses and high bandwidth. On the one hand, Asahi Kasei Company [2] and, on the other hand, Asahi Glass Company [3] in collaboration with Prof. Koike from Keio University, they both have developed different kinds of Multi-Core Polymer Optical Fibers (MCPOFs). These fibers are composed of small size cores made of polymer and embedded in a cladding material. The small cores cover as a whole the same diameter as the large core of a conventional POF; hence, the advantages of POFs are maintained whereas bending losses are reduced [4,5].

These fibers constitute a good solution not only for home networking [6] or for applications where bending losses are critical, but also for optical imaging [7]. In all these applications, a characteristic effect of MCPOFs becomes manifest: the crosstalk, which arises from the coupling phenomenon that takes place among the propagation modes of different cores of the fiber. Crosstalk can cause undesirable effects as, for instance, limiting the maximum length of an optical link or, in the case of optical imaging, impairing the quality of an endoscope by worsening the contrast and causing blurring in the final image [7]. The crosstalk is, in many instances, a non-negligible effect, as we have demonstrated in another study [8]. Hence, it is important to analyze this effect and its influence in order to perform an optimum design of an MCPOF that satisfies the requirements of a certain application.

There are many models in the literature describing crosstalk between optical fibers, but these models do not address properly the case of MCPOFs. On the one hand, there are models based on electromagnetic theory [9–13], but they are only valid for single mode fibers or for systems where only a few number of modes are excited. Since POFs are, in general, highly multimode [14], these models are not suitable for practical fibers. On the other hand, there is a quasi-ray tracing model developed by Kapany [15], and extended by Cherin and Murphy [16], which is based on analytical expressions. This model describes the crosstalk in an ordered bundle formed by a central multimode core surrounded by a ring of multimode cores, but it only takes into account meridional rays. Furthermore, the analytical expressions used to obtain the crosstalk power and output power at the end of the fiber are subjected to the constraint that only the central core is illuminated and that crosstalk can solely be produced outwards, that is, from the central core to the outer ones but not back to the central core.

In this paper we present a new ray-tracing model to describe the propagation of light in MCPOFs, taking into account the crosstalk, which definitely overcomes the limitations imposed by previous models. This new model provides us with a complete description of the ray distribution at the output end of an MCPOF regardless of which core is being illuminated at the beginning of the fiber, it takes into account not only meridional rays but also skew rays, it can be applied to MCPOFs composed of an arbitrary number of concentric rings of cores around a central core, and it calculates the crosstalk not only outwards but also backwards, that is, from the excited core (the radiating one) to the perturbed ones (the non-illuminated ones at the beginning of the fiber) and vice versa.

The structure of the paper is as follows: First, the developed ray-tracing model is explained in detail. Next, the experimental measurements and the simulations carried out

#132325 - $15.00 USD Received 27 Jul 2010; revised 10 Sep 2010; accepted 13 Sep 2010; published 8 Oct 2010

using the implemented computational model are compared in order to validate the model, and the influence of crosstalk in different MCPOFs is analyzed. Finally, the main conclusions are summarized.

2. Ray-tracing model

In this section, we present the developed ray-tracing model, which is capable of describing the propagation of light in MCPOFs by taking into account the crosstalk among adjacent cores. This model assumes that modes travelling within an individual core are uncoupled (i.e., it neglects the mode coupling between adjacent modes inside each individual core). Despite this limitation, we will still be able to make use of the model to assess the influence on crosstalk of the different parameters of the fiber. This last assertion is supported by the fact that, in another study [8], we have observed that crosstalk is much more dominant than mode coupling.

Next, the main physical mechanism that describes crosstalk among multimode individual cores, and which is known as frustrated total internal reflection, is explained and after that the ray-tracing model is presented.

2.1 Frustrated total internal reflection

When light is launched into a waveguide placed next to another one, power is transferred from one guide to the other by evanescent fields via frustrated total internal reflection [17].

Because of this mechanism, when a ray travelling within an individual core reaches the core-cladding interface, part of its power is reflected and the rest leaks outside. This leaky power can couple to a nearby fiber giving rise to crosstalk, as it is shown in Fig. 1.

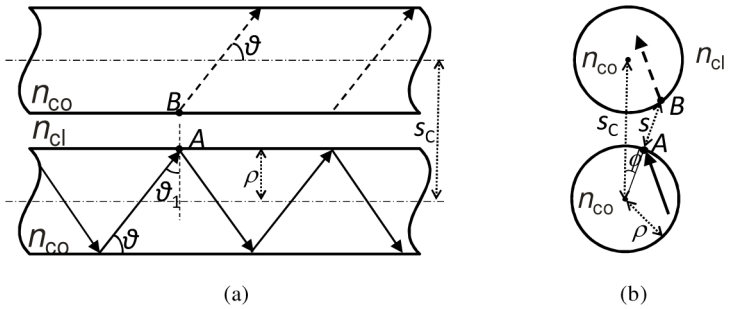

(a) (b)

Fig. 1. (a) A radiating ray travelling along the lower fiber (solid lines) gives rise to coupled rays (dashed lines) in the upper fiber. (b) Parameters of the rays projected on the cross section of a fiber bundle. n_{co} is the refractive index of the cores, n_{cl} is the refractive index of the cladding, θ is the axial angle of the ray, θ_1 is the complementary angle of the axial one, ρ is the core radius, s_C is the separation between the centers of the cores, A is the exit point of the radiating ray, B is the coupling point, s is the separation between points A and B, and ϕ is the angle between the line that joins the core centers and the line from the center of the radiating core to the point A.

The amount of power transmitted to another core at a certain turning point is given by a transmission coefficient [see Eqs. (1), (2) and (3) below], which has been calculated using plane wave incidence in three homogeneous media (core-cladding-core) [16]. The core-cladding interface can be considered as locally plane compared to the wavelength of the light [11]. It is worthy of remark that there are typographical errors in the transmission coefficient equation of Ref [16]. which, for the sake of the reader, have been corrected.

#132325 - $15.00 USD Received 27 Jul 2010; revised 10 Sep 2010; accepted 13 Sep 2010; published 8 Oct 2010

$$T(\theta,s)=\frac{1}{2}\left[\frac{1}{\cosh^2\beta+\left[\left(n_{\mathrm{cl}}^2\gamma^2-n_{\mathrm{co}}^2\cos^2\theta_1\right)/\left(2n_{\mathrm{co}}n_{\mathrm{cl}}\gamma\cos\theta_1\right)\right]^2\sinh^2\beta}\right] + \frac{1}{2}\left[\frac{1}{\cosh^2\beta+\left[\left(n_{\mathrm{cl}}^2\cos^2\theta_1-\gamma^2n_{\mathrm{co}}^2\right)/\left(2n_{\mathrm{co}}n_{\mathrm{cl}}\gamma\cos\theta_1\right)\right]^2\sinh^2\beta}\right] \quad (1)$$

$$\gamma=\left[\left(\frac{n_{\mathrm{co}}}{n_{\mathrm{cl}}}\right)^2\sin^2\theta_1-1\right]^{1/2} \quad (2)$$

$$\beta=\frac{2\pi}{\lambda}n_{\mathrm{cl}}s\gamma \quad (3)$$

In Eqs. (1), (2), and (3) n_{cl} is the refractive index of the cladding, n_{co} is the refractive index of the core, θ_1 is the complementary angle of the axial angle θ [see Fig. 1(a)] and s is the distance from the turning point (A) in the core where the ray is propagating to the coupling point (B) in the core where the ray is coupled to [see Fig. 1(b)]. In the calculations above, we are considering unpolarized light, hence the 1/2 factors on both terms on the right–hand side of Eq. (1).

The separation s is geometrically calculated in the normal direction to the core-cladding interface (i.e., in the direction of the evanescent field). Its expression is given by Eq. (4) [16]

$$s=s_{\mathrm{C}}\cos\phi-\rho-\sqrt{\rho^2-s_{\mathrm{C}}^2\sin^2\phi} \quad (4)$$

where ρ, s_{C} and ϕ are the parameters depicted in Fig. 1(b).

This way, if we arrange several cores together in a bundle (such as in the case of MCPOFs) and illuminate one of them, as a consequence of the crosstalk, not only that core will be illuminated at the output end of the bundle, but also the surrounding ones. The crosstalk power at the output end of the fiber generated by a certain ray is obtained from Eq. (5)

$$P_{\mathrm{xt}}\big|_{\mathrm{ray}}=P_{\mathrm{in}}\left[1-\left(1-T_1\right)\left(1-T_2\right)...\left(1-T_N\right)\right] \quad (5)$$

with P_{in} being the input power of the ray, T_i the transmission coefficient at the ith reflection of the ray and N the number of reflections the ray suffers along its path. Similarly, the remaining power conveyed by the ray at the output end of the fiber is given by Eq. (6)

$$P_{\mathrm{out}}\big|_{\mathrm{ray}}=P_{\mathrm{in}}\left(1-T_1\right)\left(1-T_2\right)...\left(1-T_N\right). \quad (6)$$

Notice that skew rays [11,17] have different values of the transmission coefficient T at each turning-point ($T_1 \neq T_2 \neq \ldots \neq T_N$) because the distance s changes at each reflection of the ray, as it is shown in Fig. 2(a). On the contrary, meridional rays [11,17] have the same value of the transmission coefficient at every reflection ($T = T_1 = T_2 = \ldots = T_N$) [see Fig. 2(b)].

The total amount of crosstalk can be expressed in terms of the far-end equal-level crosstalk (FEXT), which is defined by Eq. (7) [16]

$$FEXT=10\log_{10}\left(\frac{P_{\mathrm{out}}}{P_{\mathrm{xt}}}\right) \quad (7)$$

#132325 - $15.00 USD Received 27 Jul 2010; revised 10 Sep 2010; accepted 13 Sep 2010; published 8 Oct 2010

where P_{out} is the total amount of power collected at the output end of the core illuminated at the beginning of the fiber and P_{xt} is the power carried by rays in the surrounding cores. In Eq. (7) we can see that, the higher the FEXT, the lower the crosstalk is.

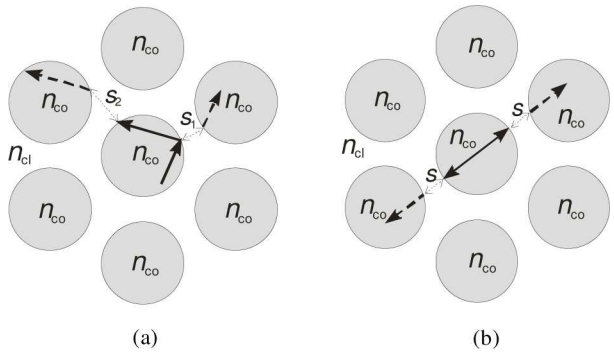

Fig. 2. (a) A skew ray (solid line) travelling in the central core gives rise to coupled rays (dashed lines) in the surrounding cores. (b) A meridional ray (solid line) travelling in the central core generates coupled rays (dashed lines) in the surrounding cores.

Once the main physical mechanism causing crosstalk has been explained, we proceed to describe the ray-tracing model we have developed.

2.2 Methodology of the ray-tracing model

Our starting point is the quasi-ray tracing model developed by Cherin and Murphy [16], as it is the most suitable for describing highly multimode fibers. This quasi-ray tracing model describes the crosstalk between a fiber and an array of fibers placed around it, such as in the case of an MCPOF with a central core surrounded by a ring of cores, as shown in Fig. 3. Nevertheless, this model has several limitations: first of all, it is based on analytical expressions which, in spite of being able to calculate the total amount of output power P_{out} and crosstalk power P_{xt} at the end of the fiber, cannot provide the power distribution of rays; secondly, it only considers meridional rays, but not skew rays, which are, in general, much more abundant [11]; thirdly, the calculated power flow always takes place from the inner cores to the outer ones, but never backwards and, finally, it is only applicable to systems formed by a central core with an array of cores placed at the same distance from this central core, that is, arranged in a ring around it. These constraints invalidate the previous model to describe MCPOFs composed of more than one ring around the central core.

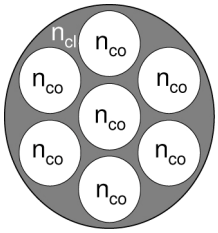

Fig. 3. Cross section of an MCPOF composed by a hexagonal array of cores, that is, a ring of six cores, around a central one.

For this reason, our aim is to develop a more complete model capable of describing crosstalk overcoming the limitations commented above. This will be explained in more detail in the following subsections.

2.2.1 A complete ray-tracing model

Our main purpose has been to include and adapt, when necessary, the analytical expressions of subsection 2.1 in a complete ray-tracing model. By considering light as a collection of

#132325 - $15.00 USD Received 27 Jul 2010; revised 10 Sep 2010; accepted 13 Sep 2010; published 8 Oct 2010

rays, such an approach allows us to obtain a ray distribution at the output end of the fiber given a ray distribution at the input end of the fiber. This way we are able to obtain not only the value of the FEXT, but also the Near-Field Pattern (NFP), the Far-Field Pattern (FFP), the fiber bandwidth and other important parameters characterizing the fiber performance.

As previously explained, when a core is illuminated in an MCPOF, the propagating rays inside this core generate, at each reflection, coupled rays in the surrounding cores. As the number of reflections is, generally, very high (in fact, it can be as high as several thousands in a one-meter-length fiber), taking into account all these rays would lead us to an intractable computational problem. Hence, it is necessary to define a criterion in order to prevent the number of rays from increasing exponentially. The adopted criterion selects only one ray between the radiating ray (i.e., the ray giving rise to crosstalk) and the coupled ray it generates when reaching the core-cladding interface. This is done according to a certain random value which will be compared to a weighted probability value assigned to each ray (one value for the radiating ray and another value for the coupled ray); this weighted probability value is proportional to the amount of ray power. This way, (1-*T*) is the probability of selecting the radiating ray whereas *T* is the probability of choosing the coupled ray. Then, the mentioned random number is generated (following a uniform distribution between 0 and 1) and, depending on its value, the following criterion is applied:

- If the random number is lower than *T*, the coupled ray is selected (being the radiating ray discarded).
- If random number is higher than *T*, the radiating ray is selected.

The selected ray holds 100% of the initial power of the ray. This process is repeated at every new reflection of the ray until it reaches the end of the fiber. This way, we obtain the resultant output power distribution given an input ray distribution at the beginning of the fiber, taking into account the crosstalk power flow not only outwards but also inwards, which overcomes two of the main limitations of the quasi-ray tracing model.

Furthermore, we take into account not only meridional rays but also skew rays (overcoming another limitation of the model developed by Cherin and Murphy). The only difference is that, when dealing with meridional rays, we solely need to calculate the transmission coefficient at the first reflection of the ray, as it will be the same at every reflection of the ray, whereas, when dealing with skew rays, the transmission coefficient has to be calculated at every reflection.

The simulations carried out using this approach have provided both accurate values of the FEXT, in excellent agreement with those obtained using the analytical expressions (as it is shown in Fig. 4) and accurate NFPs and FFPs (as will be seen in the following section). Notice that, for the sake of comparison, the simulations shown in Fig. 4 have been made employing an input ray distribution composed of only meridional rays, as the analytical expressions of the quasi-ray tracing model do not take into account skew rays.

#132325 - $15.00 USD Received 27 Jul 2010; revised 10 Sep 2010; accepted 13 Sep 2010; published 8 Oct 2010

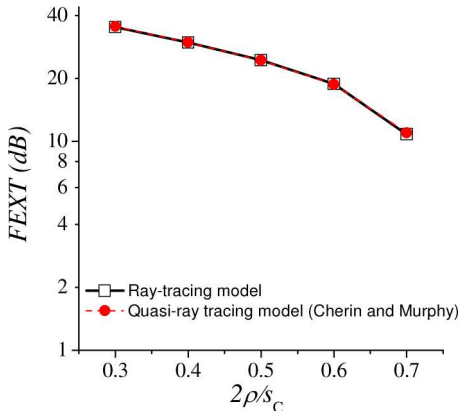

Fig. 4. Comparison of the FEXT values obtained using the ray-tracing model with those calculated evaluating the analytical expressions of the quasi-ray tracing model. The measurements have been carried out as a function of $2\rho/s_C$, being ρ the core radius and s_C the separation distance between the centers of the radiating core and of the neighboring core. The parameters used in these simulations are: 2ρ = 25.4 μm, NA = 0.1, fiber length = 1000 m and the input power distribution is $F(\theta) = \exp(-\theta/0.5\theta_C)^2$, being θ_C the critical angle, which is the maximum value of the axial angle θ in order the ray to be confined in the core.

So far, we are able to obtain an output ray distribution, provided that the MCPOF is composed of only one ring of cores around a central core. Therefore, in order to be able to simulate MCPOFs with a variable number of rings, the model must be further extended. This step will be accomplished in the following subsection.

2.2.2 Extension of the model to include a variable number of rings

As we have mentioned in the beginning of section 2, calculating the transmission coefficient T requires knowledge of the separation distance s, which is obtained from the distance s_C between the centers of the radiating core and of the neighboring core. When dealing with MCPOFs of only one ring of cores surrounding a central one, this is a relatively easy task, since all the surrounding cores are separated the same distance (s_C) from the central one. In contrast, evaluating the crosstalk for MCPOFs consisting of several rings of cores, such as that illustrated in Fig. 5, is a much more complicated task. For instance, if we label each core with i_j, being i the index of the core and j the index of the ring, we can see in Fig. 5 that the separation between the neighboring core 1_3 (or 2_3) and the core 1_2 is different from that between the neighboring core 0_2 (or 2_2) and the core 1_2.

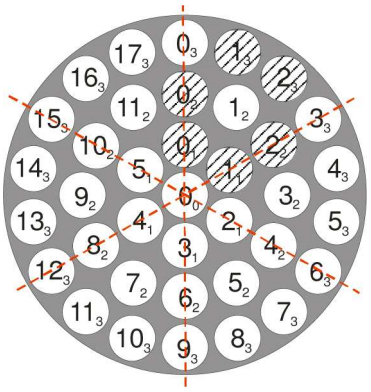

Fig. 5. Cross section of an MCPOF composed of three concentric rings of cores around a central one. The nomenclature followed to name each core is i_j, being i the index of the core and j the index of the ring. The red dashed lines mark the symmetry planes of the fiber. Hence, the core 1_2 has six neighboring cores marked with sloping lines.

#132325 - $15.00 USD Received 27 Jul 2010; revised 10 Sep 2010; accepted 13 Sep 2010; published 8 Oct 2010

In order to calculate s_C (so as to obtain the value of T), we have to distinguish between three cases:

a) When the radiating core is the innermost one, the distance from its center to the center of any of the neighboring cores in the first ring is constant and calculated according to Eqs. (8) and (9)

$$s_C = d \tag{8}$$

$$d = \frac{a-\rho}{N_{\text{rings}}} \tag{9}$$

where a is the radius of the whole fiber, ρ is the core radius and N_{rings} is the number of rings.

b) When the radiating core is in a certain ring j and crosstalk takes place to one of the two neighboring cores in the same ring, the separation distance is calculated, with the help of Fig. 6(a), by Eq. (10)

$$s_C = jd\sqrt{2\left[1-\cos\left(\Delta\varphi_j\right)\right]} \tag{10}$$

where d is obtained from Eq. (9).

c) When the radiating core is in a certain ring j and crosstalk takes place to one of the neighboring cores in a different ring k (so that $k = j + 1$ would correspond to the immediate outer ring and $k = j$-1 to the inner one), from Fig. 6(b) the separation distance is given by Eq. (11)

$$s_C = d\sqrt{2jk\left[1-\cos\left(\Delta\varphi\right)\right]+1} \tag{11}$$

where d is obtained again from Eq. (9) and $\Delta\varphi$ is the difference between the polar angles of the cores involved, as it is depicted in Fig. 6(b).

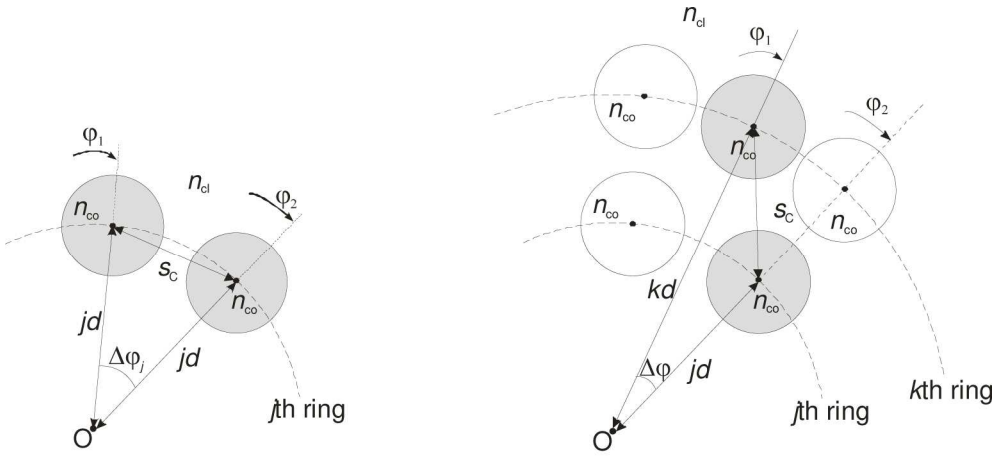

Fig. 6. Parameters for calculating the separation distance s_C between core centers (a) when crosstalk takes place to one of the two neighboring cores in the same jth ring as the radiating core, and (b) when crosstalk takes place to one of the neighboring cores of the outer kth ring (i.e. $k = j + 1$).

#132325 - $15.00 USD Received 27 Jul 2010; revised 10 Sep 2010; accepted 13 Sep 2010; published 8 Oct 2010

After having obtained the distance s_C, we only have to substitute this value into Eq. (4) and, finally, obtain the transmission coefficient T from Eq. (1).

3. Results and discussion

We have performed several experimental measurements with the aim of, on the one hand, validating our model experimentally, and, on the other hand, analyzing the influence of crosstalk in two real MCPOFs.

3.1. Characteristics of the investigated fibers

We have measured two different MCPOFs:

The first one is a prototype developed by Asahi Kasei [2], and it is composed of 37 step-index (SI) cores arranged in three concentric rings, as shown in Fig. 7. The main characteristics of this fiber, named as SI-MCPOF from now on, are shown in Table 1.

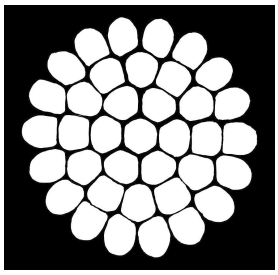

Fig. 7. Cross section of the investigated SI-MCPOF.

Table 1. Characteristics of the investigated SI-MCPOF

	Quantity	Unit
Number of cores	37	-
Core diameter	140	μm
Cladding diameter	1000	μm
Area fraction[1]	76.8	%
Numerical Aperture	0.5	-

[1]Area fraction = Core area/(Core area + Cladding area)

The second fiber under study has been manufactured by Asahi Glass [3] which is made of a perfluorinated (PF) polymer called CYTOP® and it is composed of 127 Graded-Index (GI) cores grouped together in six concentric rings around a central core, as shown in Fig. 8 (please notice that the GI refractive index makes the core-cladding boundaries to appear blurred). We will name this fiber as GI-MCPOF, and its main characteristics are summarized in Table 2.

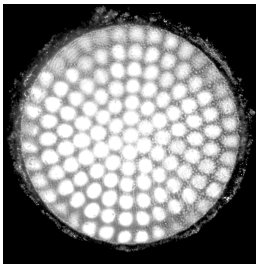

Fig. 8. Cross section of the investigated GI-MCPOF.

Table 2. Characteristics of the investigated GI-MCPOF

	Quantity	Unit
Number of cores	127	-
Core diameter	25	μm
Cladding diameter	350	μm
Area fraction	64.8	%
Numerical Aperture	0.185	-

As pointed out previously, our computational model based on the ray-tracing method is only valid for highly multimode fibers so, in order to check its suitability for describing the propagation of light in both MCPOFs, it is necessary to calculate the normalized frequency V so as to estimate the number of modes M travelling along the fiber. These values can be easily obtained in the case of an SI profile from Eqs. (12) and (13) [11]

$$V = \frac{2\pi\rho}{\lambda} NA \tag{12}$$

#132325 - $15.00 USD Received 27 Jul 2010; revised 10 Sep 2010; accepted 13 Sep 2010; published 8 Oct 2010

$$M \approx \frac{V^2}{2} \tag{13}$$

where ρ is the core radius, λ is the wavelength of the light source and NA is the maximum numerical aperture.

The values obtained in the case of the SI-MCPOF fiber using a wavelength of 594 nm (which is precisely the wavelength of the light source used in the experimental measurements explained below) are $V = 370.221$ and $M \approx 68\,532$, so it can be concluded that the behavior is multimode and, consequently, the ray-tracing model can be applied [11].

In the case of the GI-MCPOF, the value obtained for V using Eq. (12) and a wavelength of 594 nm is 24.461 and M is calculated assuming a parabolic GI profile from Eq. (14) [11].

$$M \approx \frac{V^2}{4} \tag{14}$$

Thus, $M \approx 150$, so we can conclude that the developed model can also be applied to describe the propagation of light in this second fiber [18].

3.2 Experimental set-up

The experimental set-up employed to measure the NFP and the FFP at the output end of an MCPOF is that shown in Fig. 9.

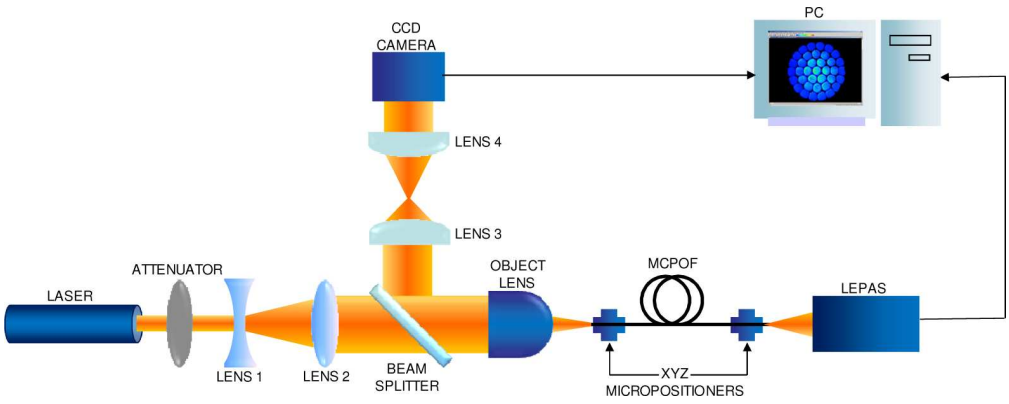

Fig. 9. Experimental set-up employed to measure the NFP and the FFP of the analyzed MCPOFs. Legend: LENS 1: symmetric-concave lens (f´ = –20 mm); LENS 2: symmetric-convex lens (f´ = + 150 mm); LENS 3: plano-convex lens (f´ = + 100 mm); LENS 4: plano-convex lens (f´ = + 50 mm); OBJECT LENS: 0.65-NA object lens.

The light source is a 594-nm-wavelength and 10 mW He-Ne laser, which is followed by an attenuator in order to avoid saturation of the CCD camera and the LEPAS optical beam measurement system [19]. The laser beam is expanded using lenses 1 and 2 so as to cover the whole aperture of the object lens placed following the beam splitter and, thus, to ensure that the whole numerical aperture of the object lens (NA = 0.65) will be covered and, consequently, all modes in both MCPOFs will be excited. This way, we will be able to analyze the crosstalk impact in the worst-case scenario. The spot size produced at the input surface of the MCPOF is 9 ± 1 μm. Since a small fraction of the light impinging on the input surface of the fiber will be reflected back to the beam splitter, we take advantage of this fact to inspect the input surface of the fiber and to control which core is illuminated. This is achieved by directing the reflected light to a CCD camera through two magnification lenses (lenses 3 and 4). In this set-up we only illuminate one core at the input of the MCPOF each time and then we measure the crosstalk power coupled to the surrounding cores at the output end (the fiber length is 1 m). The light that exits the fiber is collected by the Hamamatsu LEPAS optical beam measurement system, which allows us to measure the NFP and the FFP,

#132325 - $15.00 USD Received 27 Jul 2010; revised 10 Sep 2010; accepted 13 Sep 2010; published 8 Oct 2010

and, consequently, the value of the FEXT by dividing the power received from the core excited at the beginning of the fiber by the total amount of power collected from the rest of the cores.

3.3 Near- and Far-Field Patterns and FEXT calculations

In this subsection we will analyze the results obtained from the simulations and the experimental measurements performed on the fibers described above. The obtained results are the NFP, the FFP, and the FEXT at the end of a 1-m-length fiber.

3.3.1 Results for the SI-MCPOF

Figure 10 shows the NFP and the FFP obtained when only the core 0_0 (the central one) of the SI-MCPOF is excited. Observing the NFP, we can see that crosstalk is not very noticeable (both in the experimental measurement and in the simulation), as there is almost no power in the cores surrounding the central one. Furthermore, the measured value of the FEXT is 16.04 dB and the simulated one is 16.14 dB. The excellent agreement between the simulated and measured values serves us to validate the applicability of the model in obtaining the amount of crosstalk produced in an SI-MCPOF. However, a closer inspection reveals that in the simulated NFP most of the power is confined in the central region of the illuminated core. This is explained by the fact that the simulated fiber is ideal (mode coupling has been neglected) and, since the launching light spot is very small (resembling 9 μm spot size of the experimental set-up), the short length of this fiber is insufficient for the calculated ray power to redistribute about the whole core, so that in the calculated NFP the power keeps confined in the center of the illuminated core. In contrast, the presence of inhomogeneities in real fibers gives rise to mode coupling, favoring the redistribution of light power along the core, which explains the smoother power distribution of the illuminated core in the experimentally measured NFP.

In addition, the FFPs obtained in both simulation and experimental measurements agree quite well, since both extend to the same limit acceptance angles [see Figs. 10(c) and (d)]. As to their pattern, we can observe that the simulated FFP has a rather uniform pattern (due to the SI profile of the cores), whereas the experimental FFP shows a more Gaussian-like pattern. This can be explained in terms of the differential mode attenuation, which makes higher order modes attenuate faster than lower order modes; this would explain why the measured power is lower at higher far-field angles. This effect is not observed in the simulated FFP because we are dealing with ideal fibers.

#132325 - $15.00 USD Received 27 Jul 2010; revised 10 Sep 2010; accepted 13 Sep 2010; published 8 Oct 2010

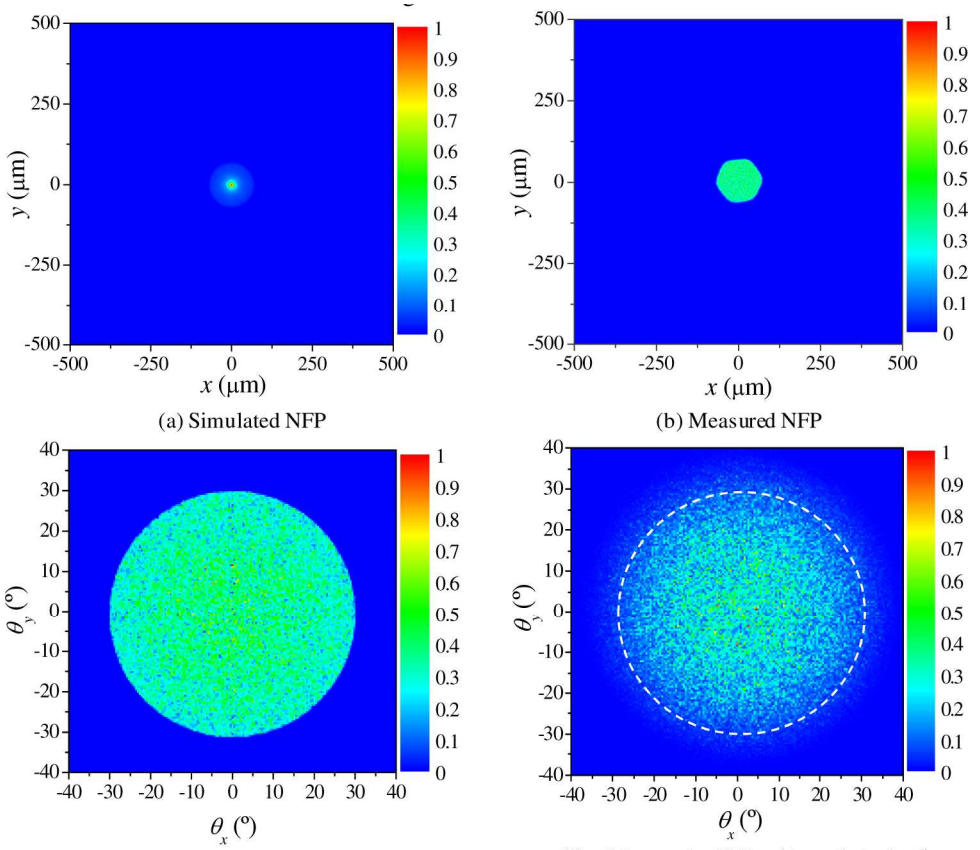

Fig. 10. Normalized NFP and FFP obtained at the end of a 1 m SI-MCPOF when only the core 0_0 is excited.

Due to the geometry of the cross section of the fiber, not all the cores in an SI-MCPOF undergo the same amount of crosstalk, as the arrangement of the surrounding cores is not the same for all cores. This makes the FEXT to change depending on which core is being illuminated at the beginning of the fiber. To illustrate this point we have made another measurement exciting the core 7_2, which is the one having the largest separation distance with respect to its neighboring cores, in contrast to the core 0_0, which is the one having the smallest separation distance. The obtained results for the NFP and FFP are shown in Fig. 11. In this case, the FEXT value obtained from the simulated NFP is 31.28 dB, whereas the experimental one is 17.32 dB. There is little difference between the experimental value obtained for the core 0_0 and that corresponding to the core 7_2, but there is quite a big difference between the simulated values. We attribute this discrepancy to the different shape of the cores in the real fiber compared to the ideal (simulated) one (cf. Fig. 7 with Fig. 5). The shape of the cores in the real SI-MCPOF is practically hexagonal (instead of being circular, due to some effect during the manufacturing process [20]), which packs them tighter in a similar fashion to a honeycomb, reducing the gap between them. As a consequence, the crosstalk increases, reducing the value of the FEXT; in fact, we have checked that the experimental value of the FEXT is practically the same for all cores in the real fiber, being always in the range of 16 dB regardless of the excited core. With regard to the FFPs, they agree quite well, since both extend to the same limit acceptance angles [Figs. 11(c) and 11(d)].

#132325 - $15.00 USD Received 27 Jul 2010; revised 10 Sep 2010; accepted 13 Sep 2010; published 8 Oct 2010

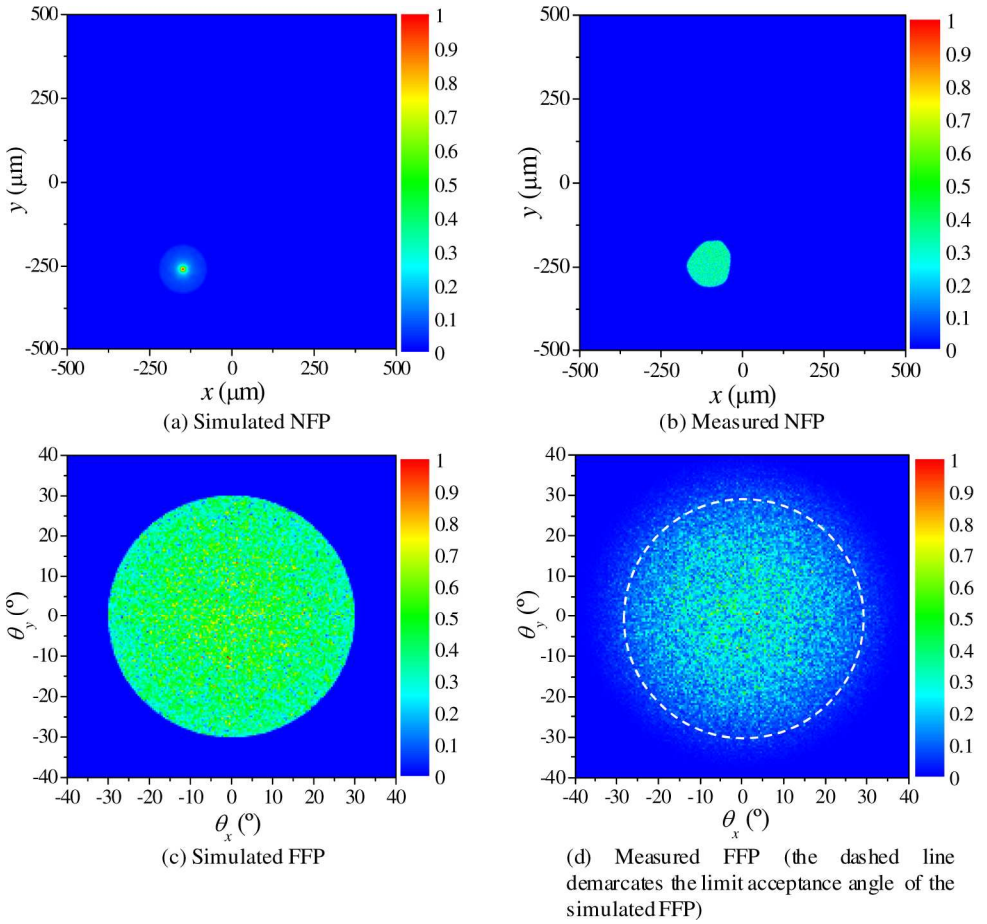

Fig. 11. Normalized NFP and FFP obtained at the end of a 1 m SI-MCPOF when only the core 7_2 is excited.

3.3.2 Results for the GI-MCPOF

At this point, it is important to stress on the fact that the simulation results obtained for the GI-MCPOF are only intended as a first approach, and that they should not be regarded as a substitute for the experimental measurements, but as a complement to them, due to the constraint that, for the time being, our computational tool simulates MCPOFs composed of only SI cores. However, we can still obtain valuable information from the simulations about the influence of the different characteristics of the GI-MCPOF on crosstalk, such as the NA or the core radius, and compare them with the characteristics of the SI-MCPOF.

Let us now discuss the obtained results: the NFPs and the FFPs obtained when only the core 0_0 is illuminated are shown in Fig. 12.

We can see that, in both simulated and measured NFPs, the most powerful cores at the end of the fiber are those placed in the symmetry planes of the fiber because, since the distance s between these cores is smaller, the transmission coefficient T is higher and so it is the crosstalk. In spite of the good qualitative agreement between the simulated and measured NFPs, there are quantitative differences, since the FEXT value obtained from the simulated NFP is −5.78 dB, while the value obtained from the measured one is −1.47 dB, leading to a lower crosstalk than expected. The disagreement can be explained by the limitation previously explained, i.e. that the simulation has been carried out for an SI profile instead of a GI profile; indeed, in a GI profile, rays curve before reaching the core-cladding interface [11],

#132325 - $15.00 USD Received 27 Jul 2010; revised 10 Sep 2010; accepted 13 Sep 2010; published 8 Oct 2010

reducing the crosstalk and, therefore, increasing the FEXT. This is better appreciated in the FFPs shown in Figs. 12(c) and 12(d): in the experimental FFP, most of the power collected is conveyed by rays propagating at low values of the axial angle due to the GI profile of the cores, whereas the simulated FFP has a more uniform pattern extending to higher acceptance angles. However, in spite of these discrepancies, these results are still valuable because they can be used to compare the differences in both kinds of fibers investigated in this paper.

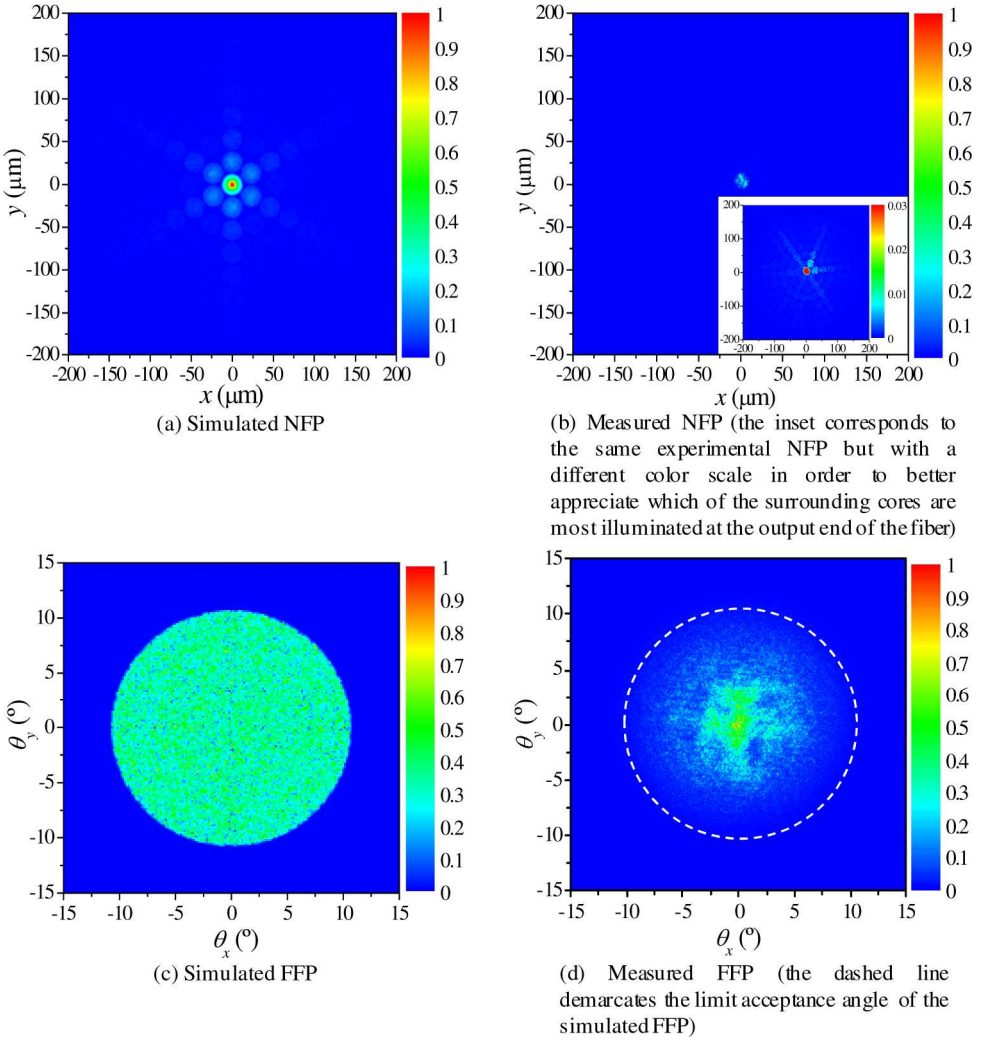

(a) Simulated NFP

(b) Measured NFP (the inset corresponds to the same experimental NFP but with a different color scale in order to better appreciate which of the surrounding cores are most illuminated at the output end of the fiber)

(c) Simulated FFP

(d) Measured FFP (the dashed line demarcates the limit acceptance angle of the simulated FFP)

Fig. 12. Normalized NFP and FFP obtained at the output of a 1 m GI-MCPOF when only the core 0_0 is excited.

For instance, we can observe in the experimental measurements that, when the central core is illuminated, the crosstalk generated in the GI-MCPOF is higher than in the SI-MCPOF (−1.47 dB of the GI-MCPOF against 16.04 dB of the SI-MCPOF). That can be justified attending to the different NA of the fibers. Indeed, from the theoretical expressions it can be easily deduced that, the greater the NA, the smaller the crosstalk is [5,16], so that, as the NA of the GI-MCPOF is much lower than that of the SI-MCPOF, a much higher crosstalk is observed. However, the reader is cautioned that, although a lower crosstalk could seem attractive, increasing the NA involves a decrease in bandwidth [5]. We have also observed that, as expected, the amount of crosstalk is inversely proportional to the separation between

#132325 - $15.00 USD Received 27 Jul 2010; revised 10 Sep 2010; accepted 13 Sep 2010; published 8 Oct 2010

the rings of cores. Thus, since the SI-MCPOF has a larger ring separation than the GI-MCPOF (so that the distance *s* is larger), the crosstalk is lower in the former. Another parameter which has an impact on the crosstalk is the core radius due to the fact that smaller core sizes imply an increase in the number of reflections and, consequently, a further increase in the crosstalk. That behavior is indeed what we observe when we compare the results of both fibers, i.e. the crosstalk is lower in the case of the SI-MCPOF which has larger cores. Even though reducing the crosstalk is in most instances desirable, it is important to keep in mind that increasing the core radius means increasing bending losses [21,22] whereas increasing the NA leads to lower bandwidth [5], a fact that would eventually counteract the main advantages of MCPOFs. Therefore, an increase in the radius of each core or in the numerical aperture in the search of lower crosstalk should be applied cautiously.

As it has been done in the case of SI-MCPOF, we have made another measurement illuminating the core with the largest distance to its neighboring cores (core 22_4). The obtained results for the NFP and the FFP are shown in Fig. 13.

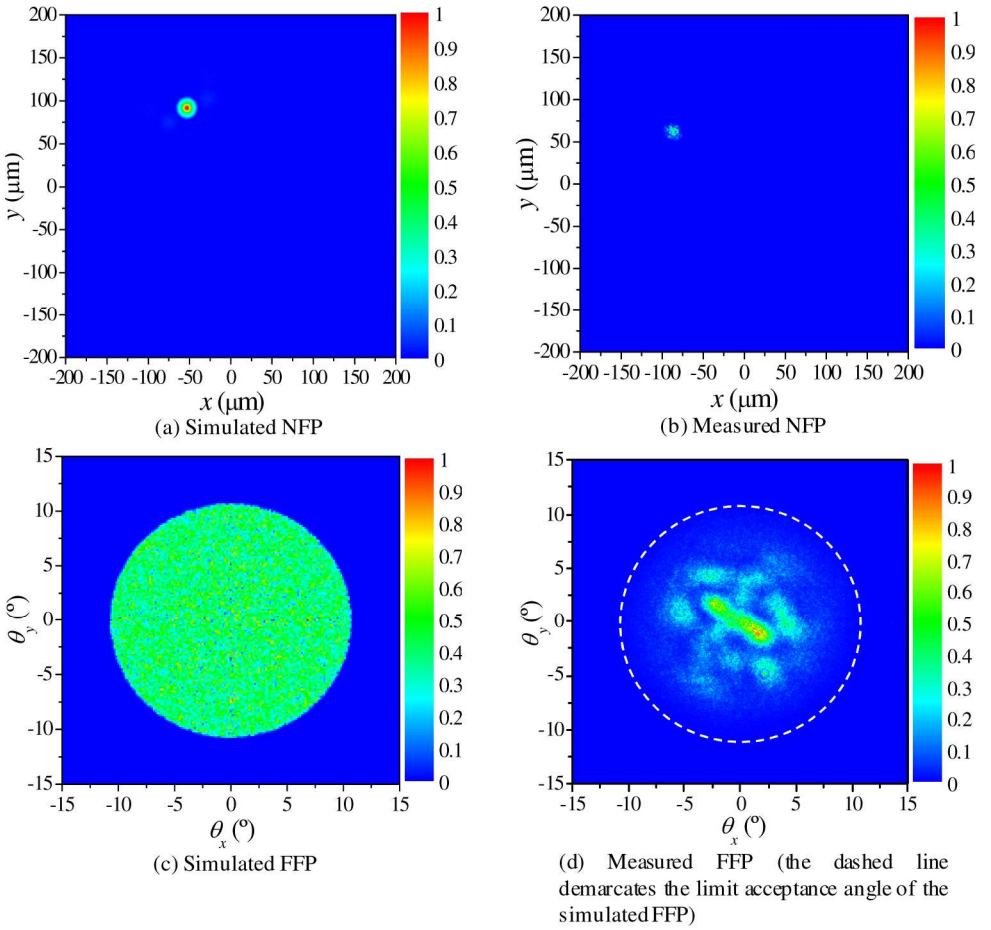

Fig. 13. Normalized NFP and FFP obtained at the output of a 1 m GI-MCPOF when only the core 22_4 is excited.

In that case, the crosstalk is not as high as in the case when the core 7_2 of the SI-MCPOF was excited. That becomes clear in the FEXT values obtained from the simulated and experimental NFPs, being those values 2.55 dB and 3.55 dB respectively. In addition, the difference between FEXT values measured when exciting core 0_0 and core 22_4 is larger than the difference obtained in the case of the SI-MCPOF. The reason for that behavior lies mainly

#132325 - $15.00 USD Received 27 Jul 2010; revised 10 Sep 2010; accepted 13 Sep 2010; published 8 Oct 2010

on the shape of the cores, which are circular in the case of the GI-MCPOF and practically hexagonal in the case of the SI-MCPOF. Hence, depending on the illuminated core at the beginning of the fiber, the amount of measured crosstalk varies noticeably. Again, the simulated value is more pessimistic than the measured one, even though we observe a qualitative decrease in both cases in comparison with the values obtained when the core 0_0 was excited.

All in all, these results suggest that, despite being inadequate to provide a quantitative estimate of the crosstalk in GI-MCPOFs, the simulation results still serve as a guide to predict in which core the light excitation leads to higher or lower crosstalk.

4. Conclusions

We have developed a new ray-tracing model that deals with crosstalk and overcomes many of the limitations of previous theoretical approaches available in the literature, providing us with a complete description of the ray distribution at the output end of the fiber regardless of which core is being excited. The model, which takes also into account skew rays, can be applied to MCPOFs composed of an arbitrary number of rings, and it calculates the crosstalk both outwards and inwards.

The model developed by us is suitable to estimate the amount of crosstalk and the FFP and the NFP of MCPOFs, provided that the nonuniformities of real fibers are not significant. Our computational tool allows us to obtain the crosstalk in MCPOFs of different characteristics, such as different numerical aperture, core radius, number of cores, and so on, which could help the designers to analyze the influence of each parameter on crosstalk.

From the comparison of the experimental results obtained for two different prototypes of MCPOFs, we have concluded that both the numerical aperture and the radius of each individual core have a great influence on the crosstalk. Thus, crosstalk could be reduced by increasing the core radius and the numerical aperture, although, it is important to keep in mind that these actions would also increase the bending losses or lead to the reduction of the bandwidth, respectively. Interestingly, the different sets of experimental measurements carried out in the investigated fibers have also revealed that the amount of crosstalk varies substantially depending on which core is being illuminated at the beginning of the fiber.

Acknowledgments

This work was supported by the institutions Ministerio de Ciencia e Innovación, Universidad del País Vasco/Euskal Herriko Unibertsitatea, and Gobierno Vasco/Eusko Jaurlaritza, under projects TEC2009-14718-C03-01, GIU05/03 and UE08-16, and AIRHEM and S-PE09CA03, respectively. The research leading to these results has also received funding from the European Commission's Seventh Framework Programme (FP7/2007-2013) under grant agreement no. 212912. One of the authors has a research fellowship from Vicerrectorado de Investigación, Universidad del País Vasco/Euskal Herriko Unibertsitatea, while working on her PhD.

#132325 - $15.00 USD Received 27 Jul 2010; revised 10 Sep 2010; accepted 13 Sep 2010; published 8 Oct 2010